Biochimica et Biophysica Acta 1812 (2011) 1393–1402

Contents lists available at ScienceDirect

Biochimica et Biophysica Acta

journal homepage: www.elsevier.com/locate/bbadis

Glucose-6-phosphate isomerase deficiency results in mTOR activation, failed translocation of lipin 1α to the nucleus and hypersensitivity to glucose: Implications for the inherited glycolytic disease

Jorge F. Haller [a], Sarah A. Krawczyk [b], Lubov Gostilovitch [a], Barbara E. Corkey [b], Raphael A. Zoeller [a,*]

[a] Department of Physiology and Biophysics, Boston University School of Medicine, USA
[b] Department of Medicine and Biochemistry, Boston University School of Medicine, USA

ARTICLE INFO

Article history:
Received 6 December 2010
Received in revised form 10 July 2011
Accepted 12 July 2011
Available online 23 July 2011

Keywords:
Glucose-6-phosphate isomerase deficiency
Mutant
Phospholipid biosynthesis
Lipin 1
Lipodystrophy
Non-spherocytic anemia

ABSTRACT

Inherited glucose-6-phosphate isomerase (GPI) deficiency is the second most frequent glycolytic erythroenzymopathy in humans. Patients present with non-spherocytic anemia of variable severity and with neuromuscular dysfunction. We previously described Chinese hamster (CHO) cell lines with mutations in GPI and loss of GPI activity. This resulted in a temperature sensitivity and severe reduction in the synthesis of glycerolipids due to a reduction in phosphatidate phosphatase (PAP). In the current article we attempt to describe the nature of this pleiotropic effect. We cloned and sequenced the CHO lipin 1 cDNA, a gene that codes for PAP activity. Overexpression of lipin 1 in the GPI-deficient cell line, GroD1 resulted in increased PAP activity, however it failed to restore glycerolipid biosynthesis. Fluorescence microscopy showed a failure of GPI-deficient cells to localize lipin 1α to the nucleus. We also found that glucose-6-phosphate levels in GroD1 cells were 10-fold over normal. Lowering glucose levels in the growth medium partially restored glycerolipid biosynthesis and nuclear localization of lipin 1α. Western blot analysis of the elements within the mTOR pathway, which influences lipin 1 activity, was consistent with an abnormal activation of this system. Combined, these data suggest that GPI deficiency results in an accumulation of glucose-6-phosphate, and possibly other glucose-derived metabolites, leading to activation of mTOR and sequestration of lipin 1 to the cytosol, preventing its proper functioning. These results shed light on the mechanism underlying the pathologies associated with inherited GPI deficiency and the variability in the severity of the symptoms observed in these patients.

1. Introduction

Glucose-6-phosphate isomerase (GPI, EC 5.3.1.9) is a cytosolic, non rate-limiting enzyme in glycolysis. It catalyzes the reversible isomerization of glucose-6-phosphate to fructose-6-phosphate. Mutations in GPI are the second most frequent cause of inherited glycolytic enzymopathy in humans [1]. This autosomal recessive disorder is characterized by a non-spherocytic anemia of variable severity which can present with neuromuscular dysfunctions defined by muscle weakness and mental retardation [2]. Patients and mice with the same GPI mutations can have different outcomes in the severity of the anemia or the neuromuscular dysfunction [2–4]. Unfortunately, the mechanism by which GPI deficiency causes these symptoms is not well understood [1,2]. Hence, the current therapeutics for these patients involve splenectomy and blood transfusions reserved for the most severe hemolytic cases [1,2].

We have recently isolated three independent CHO (Chinese hamster ovary) derived cell lines, each of which presented a different point mutation in GPI [5]. These cell lines displayed low GPI activity, were all deficient in the synthesis of glycerolipids, and had decreased phosphatidate phosphatase (PAP, EC 3.1.3.4) activity (Fig. 1). They also presented a temperature sensitive phenotype; these cells were unable to grow at 40 °C [5]. Expression of wild-type GPI in these cells recovered glycerolipid biosynthesis and PAP activity and corrected the temperature dependent phenotype, demonstrating a dependence of PAP activity and glycerolipid biosynthesis on GPI activity through an, as yet, unknown mechanism.

PAP is crucial for animal cell glycerolipid biosynthesis, catalyzing the dephosphorylation of phosphatidic acid (PA) to form diacylglycerol (DAG), which is required for the de novo synthesis of phosphatidylethanolamine (PE), phosphatidylcholine (PC) and triglycerides (TG)

Abbreviations: GPI, glucose-6-phosphate isomerase; G6P, glucose-6-phosphate; F6P, fructose-6-phosphate; PAP, phosphatidate phosphatase; PA, phosphatidic acid; DAG, diacylglycerol; PE, phosphatidylethanolamine; PC, phosphatidylcholine; TG, triglycerides; PPAR, peroxisome proliferator-activated receptor; CHO, Chinese hamster ovary; mTOR, mammalian target of rapamycin; $^{32}P_i$, [^{32}P]orthophosphate; GFP, green fluorescent protein; FBS, fetal bovine serum; PDK1, phosphoinositide-dependent kinase-1; S6K, S6 Kinase; AMPK, adenosine monophosphate activated protein kinase; PI3K, phosphoinositide 3-kinase; GSK-3β, glycogen synthase kinase 3 beta; PTEN, phosphatase and tensin homolog; NHSA, non-spherocytic hemolytic anemia

* Corresponding author at: 700 Albany St. W-302 Boston University, Boston, MA 02215. Tel.: +1 617 638 4010; fax: +1 617 638 4041.
E-mail address: rzoeller@bu.edu (R.A. Zoeller).

0925-4439/$ – see front matter © 2011 Elsevier B.V. All rights reserved.
doi:10.1016/j.bbadis.2011.07.007

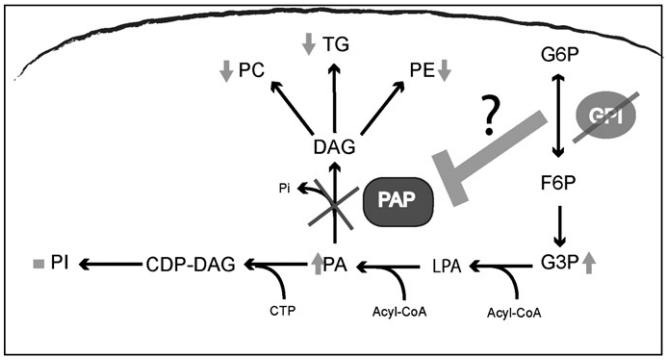

Fig. 1. Schematic diagram of pathways involving PAP and GPI in mammalian cells. GPI catalyzes the reversible conversion of G6P to F6P in the second step of glycolysis. We previously described three GPI-deficient mutant cell lines that also presented deficiencies in PAP activity [5]. This activity is required for the dephosphorylation of PA to supply DAG in the de novo biosynthesis of PC, PE and TG. As a result, the mutant cell lines presented a severe reduction in the synthesis of PC, PE and TG, accompanied by an accumulation of PA and G3P with no changes in the synthesis of PI (synthesized independently of PAP). The exact nature of the relationship between GPI and PAP is not yet understood. Abbreviations: GPI, glucose-6-phosphate isomerase; G6P, glucose-6-phosphate; F6P, fructose-6-phosphate; PAP, phosphatidate phosphatase; G3P, glycerol-3-phosphate; PA, phosphatidic acid; LPA, lysophosphatidic acid; DAG, diacylglycerol; CDP-DAG, CDP-diacylglycerol; PI, phosphatidylinositol; PC, phosphatidylcholine; PE, phosphatidylethanolamine; TG, triglycerides; P_i, inorganic phosphate.

(Fig. 1). This activity is encoded for, in mammals, by the lipin genes (*Lpin 1*, *Lpin 2*, and *Lpin 3*) [6,7] which share high sequence identity and belong to the HAD superfamily of phosphatases. All lipins contain a nuclear localization signal (NLS), which targets certain isoforms to the nucleus [8]. It is thought that these proteins have dual functionality [9]; in the cytoplasm they act as phosphatases involved in glycerolipid biosynthesis [7], while in the nucleus they are co-transcriptional factors, binding to members of the PPAR family as well as other nuclear receptors such as hepatocyte nuclear factor 4α, estrogen receptor α and the glucocorticoid receptor [9].

Of the lipins, lipin 1 is the most studied. Lipin 1 is expressed as two alternative splice isoforms, lipin 1α and lipin 1β. Lipin 1α localizes mainly to the nucleus, while lipin 1β, which has an extra 33–37 amino acid insert and is targeted almost exclusively to the cytoplasm [10,11]. PAP/lipin 1 localization and activity are regulated through phosphorylation, with at least 19 phosphorylation sites identified by mass spectrometry [10]. It is likely that hyperphosphorylation, due to mTOR signaling, results in lipin 1α not localizing to the nucleus and lipin 1β not associating with membranes, where its substrate is located and synthesis of glycerolipids occurs [12]. Phosphorylation of lipin 1 has been shown to occur in a rapamycin-inhibitable manner [12,13], implicating the mTOR complex in the regulation of lipin 1 [10,12,13].

Similar to GPI deficiencies, inborn errors in lipin genes result in pathologies in humans and mice. For example, a point mutation in lipin 1 causes a severe lipodystrophy and neuropathies due to a demyelization in the homozygous mutant mice [14,15] as well as myopathies in children due to an alteration in the phospholipid composition of the skeletal muscle fiber membranes [16]. Mutations in the lipin 2 gene are the cause of severe anemia in Majeed Syndrome [17].

In the present study we describe the cloning of lipin 1α and lipin 1β from the wild-type CHO cell line. We examined the subcellular distribution and effect of expression of these isozymes in the parent and GPI-deficient CHO strains. We found that GPI-deficient cells mislocalized lipin 1α to the cytosol, presented an abnormal, activated mTOR signaling pathway and were hypersensitive to glucose. Altogether, the data presented here serves to explain the dependency of PAP activity on GPI and sheds light on the mechanism of the pathophysiological state of GPI-deficient cells and the variability in the degree of severity of the symptoms in GPI-deficient patients.

2. Material and methods

2.1. Materials

^{32}P-inorganic phosphate ($^{32}P_i$) was obtained from Perkin Elmer/New England Nuclear. Lipids were purchased from Avanti Polar Lipids. Silica gel G and silica gel 60 thin-layer chromatography plates (EMD), Ham's F12 and DMEM medium (Cellgro or Gibco), fetal bovine serum (HyClone) and tissue culture dishes were obtained from Fisher Scientific. Antibodies were purchased from Cell Signaling with the exception of anti-actin (catalog no. MS-1295, Thermo Scientific). All other reagents, unless otherwise specified, were purchased from Sigma-Aldrich.

2.2. Cell lines and cell culture conditions

If not specified otherwise, cells were maintained in Ham's F12 medium supplemented with 10% fetal bovine serum, 1 mM glutamine, penicillin G (100 U/ml) and streptomycin (75 U/ml). Cells were cultured at 33 °C or 40 °C using 5% CO_2. Cell lines used were ZR-82 [18], a peroxisome-deficient strain derived from wild-type CHO-K1; GroD1, a GPI mutant and glycerolipid deficient cell line derived from ZR-82 [5]; and, GroD1$^{t(GPI)}$ a stable GroD1 cell population expressing wild-type hamster GPI [5].

2.3. Cloning and sequencing of hamster lipin 1

Total RNA was isolated from cells with the RNeasy kit (Qiagen) and first strand synthesis of RNA was performed with SuperScript III reverse transcriptase (Invitrogen). Hamster lipin 1 was cloned from CHO-K1, ZR-82 and GroD1 cells from total cDNA using primers designed for regions of high homology among known lipin cDNA's at either end of the cDNA; forward 5′ ATG AAT TAC GTG GGG CAG 3' and reverse primer 5′ CCA GGG TCC CCA CAA CCT ATC CTT TAA T 3'. Once the PCR product was obtained, the initial sequences were obtained with primers used to generate the PCR product. As new sequences for hamster lipin 1 were obtained, new primers were designed to sequence the entire cDNA. Digestion of the β isoform from the PCR product was performed with Ale I (New England Biolabs) to allow sequencing of lipin 1α. CHO-K1 lipin 1α and lipin 1β were cloned into the pSC vector using a blunt PCR cloning kit from Stratagene. cDNA sequences for hamster lipin 1β beta and lipin 1α were submitted to the NHI GenBank sequence database, accession numbers GU474204 and GU474205 respectively.

2.4. Expression of hamster lipin 1

For stable mammalian expression, lipin 1 was cloned using the forward primer 5′ GTT GTT GAA TTC CAC CAA TGA ATT ACG TGG GGC AGT T 3′ and reverse primer 5′ GTT GTT GAA TTC AGT GGT GAT GGT GAT GAT GAG CTG AGG CTG AAT TGT ACG T 3′ and inserted as an EcoRI fragment into the pBABEpuro vector [19] to generate pBABE(Lpin1α)puro and pBABE(Lpin1β)puro vectors. HEK293T cells were co-transfected with helper virus pCL-10A1 (Imgenex) and pBABEpuro vectors, using Fugene 6 (Roche) to produce supernatant rich in non-replicative retroviral particles. Cells were infected for 3 h with virus containing supernatant in the presence of 10 μl/ml polybrene. Medium was changed to Ham's F12 containing 10% FBS and 6 μg/ml puromycin 24 h post infection.

2.5. Phospholipid biosynthesis

For phospholipid biosynthesis, short-term labeling with $^{32}P_i$ was used. Cells were plated into six well tissue culture plates (2.5×10^5 cell/well) and allowed to attach overnight at 33 °C. The next day, vials were placed at 40 °C for 2 h, medium was then changed to growth medium containing $^{32}P_i$ (20–50 μCi/ml) and incubated for 2.5 to 3 h at 40 °C.

These times have been chosen because they've been shown to be within the linear range for ^{32}P-labeling of phospholipids in CHO cells [18]. Medium was removed and lipids were extracted accordingly to the method of Bligh and Dyer [20] in the presence of 300 μg carrier lipid (total bovine heart extract). An aliquot was taken to determine total chloroform-soluble radioactivity. Phospholipids were separated by two-dimensional thin-layer chromatography (2D TLC) using silica gel 60 plates as described [5]. Individual phospholipid species were located by autoradiography and co-migration with authentic standards. Radioactive bands were scraped and radioactivity was quantitated using liquid scintillation spectrometry. Parallel, unlabeled wells were used for protein determinations.

2.6. Measurement of neutral lipid levels

Cells were plated in 100 mm diameter tissue culture dishes at 10^6 cells/dish and allowed to attach overnight at 33 °C. The next morning, the medium was changed to Ham's F12 media containing 10% FBS and 100 μM oleic acid (2:1 FA:albumin ratio). Cells were grown at 37 °C for 48 h after which they were harvested with trypsin, resuspended in PBS and lipids were extracted as described above. Neutral lipids were separated using single dimension TLC on silica gel G plates using hexane:ethyl ether:acetic acid (70:30:1; v/v) as the development system. Plates were charred on a hot plate after spraying the plate with 50% sulfuric acid. Charred plates were scanned and the densities of the bands of interest were determined using the National Institute of Health ImageJ program [21]. Quantitation was performed by comparison to standard curve for each neutral lipid class, run in adjacent lanes on the same TLC plate.

2.7. Phosphatidate phosphatase activity assay

PAP activity was measured in the soluble fraction of whole-cell homogenates obtained by ultracentrifugation of a sonicated lysate [5]. [^{32}P]PA was synthesized enzymatically, using diacylglycerol kinase, diolein and [γ-^{32}P]ATP as described previously [22]. PAP activity was measured by following the release of water-soluble $^{32}P_i$ from chloroform-soluble [^{32}P]PA for 20 min at 37 °C. The reaction mix contained 50 mM Tris-maleate buffer (pH 7.0), 2 mM $MgCl_2$, 0.1 mM [^{32}P]PA (10,000 cpm/nmol), 0.5 mM trition X-100, and cellular protein (~25 μg) in a total volume of 0.1 ml. Mg^{2+}-dependent PAP activity represents the difference in activity obtained with or without the addition of 5 mM EDTA to the assay mixture. All enzyme assays were conducted in triplicate and were linear with time and protein concentration.

2.8. Fluorescence localization of lipin 1

Hamster lipin 1 isoforms were cloned into the pcDNA3.1-Ct-GFP vector using the TOPO TA cloning kit (Invitrogen). The forward primer 5′ GAC CAT GAA TAC GTG GGG CAG 3' and reverse primer 5′ CTG AGG CAG AAT GA TGT CC ′3 were used. Sequence directionality and correct frame sequence with GFP were verified by sequencing. This results in a GFP at the carboxy terminus of the lipin 1 polypeptide. Cells (10^5 cells/dish) were plated into 35-mm diameter poly-d-lysine glass cover (No. 1.0) bottom tissue culture dishes (catalog no. P35GC-1-14-C, MatTek Corporation) in 2 ml of Ham's F12 media containing 10% FBS. The next day, cells were transfected with 2 μg of plasmid DNA and 6 μl of Fugene 6 (Roche) following the manufacturer's protocol. For some samples, medium was switched 4 h after transfection to medium containing 50 nM rapamycin or 30% FBS and 4 mM glucose. Cells were observed 24 h post-transfection with a Nikon deconvolution inverted epiflourescent microscope. Just prior to observation, Hoechst 33342 (Invitrogen) fluorescent nuclear stain (final concentration of 0.1 μg/ml) was added.

2.9. Coomassie blue staining of colonies

Cell growth was visualized by staining cell colonies with Coomassie blue [23]. Briefly, cells were plated at low density (500 cells/well) in 24-well dishes and grown for 12 to 14 days in the specified medium. Medium was removed, cells were rinsed twice with PBS (phosphate-buffered saline), then stained with 0.5% Coomassie blue in methanol: water: acetic acid (45:45:10; v/v) for 1 h, followed by three washes of 10 min each with methanol: water: acetic acid (45:45:10; v/v) and allowed to dry prior to digitalization of the plates using a commercial desktop scanner.

2.10. Measurement of glucose-6-phosphate and fructose-6-phosphate levels

Cellular glucose-6-phosphate (G6P) and fructose-6-phosphate (F6P) levels were measured enzymatically by measuring NADPH fluorescence as described by Lang and Michal [24]. Briefly, cells from five confluent 100 mm diameter dishes were harvested with trypsin and pelleted by centrifugation at 1000×*g* for 5 min. Metabolites were then extracted on ice with 1 ml of 0.8% perchloric acid. The extraction was neutralized with 10 M KOH to pH 7 and 500 μl aliquots were assayed. The final assayed contained 0.2 N triethanolamine buffer (pH 7.5), 5 mM $MgCl_2$, 20 μM $NADP^+$ in a final volume of 1 ml. Glucose-6-phosphate dehydrogenase (0.06 units) was added to measure glucose-6-phosphate. After complete depletion of G6P in the sample, 0.035 units of commercial glucose-6-phosphate isomerase was added to measure fructose-6-phosphate. Known concentrations of either G6P or F6P were added to the samples to allow for quantification.

2.11. SDS PAGE and Western blotting

Cells were plated in 6 well plates at 80,000 cells/well in 2 ml of medium and allowed to attach overnight at 33 °C. The next day cells were shifted to 40 °C for 24 h. Cells were then washed with ice-cold PBS and lysed in RIPA buffer (50 mM Tris-HCl pH 7.4, 150 mM NaCl, 0.5% sodium deoxycholate, 0.1% SDS, 1% NP-40) in the presence of Halt protease and phosphatase inhibitor cocktail (Thermo Fischer Scientific). Samples were resolved by electrophoresis using a 9% SDS-PAGE and electro-transferred onto a polyvinylidene difluoride membranes overnight. Membranes were blocked in 5% non-fat milk in TBST (20 mM Tris-HCl, pH 8.5, 150 mM NaCl, 0.5% Tween) at room temperature for 2 h. Blots were incubated at 4 °C with primary antibody (1:1000) overnight in 5% bovine serum albumin in TBST. Membranes were washed three times for 15 min in TBST followed by incubation with the appropriate horse radish peroxidases-couple secondary antibody (catalog no. AP123P, Chemicon) for 1 h at room temperature. Membranes were washed and visualized with enhanced chemiluminescent reagent (ECL, Thermo Scientific) and X-ray film. Membranes were subsequently stripped using Restore Western Stripping Solution (Thermos Scientific) or by incubating membranes with 50 mM Tris-HCl pH 6.8, 2% SDS and 0.71 M β-mercaptoethanol at 50–60 °C 30 min and then re-probed for loading controls as indicated. Radiograph signal intensities were quantified using the National Institute of Health ImageJ software [21].

2.12. Lipin 1β gel shift

Cells were transfected with the lipin 1β-GFP construct used for fluorescent lipin 1 localization experiments described above. After 48 h, cell lysates were resolved on a 10% acrylamide TXG gel (Biorad) at 200 volts for 2 to 3 h, electro-transferred to a membrane which was probed using primary antibody against GFP (Invitrogen) as described above.

2.13. Protein determination

Protein determinations were performed using the BCA kit and Coomassie protein assay reagent (Thermo Fisher Scientific).

2.14. Statistical analysis

For comparison of multiple samples ANOVA, followed by Tukey's HSD multiple comparison procedure was performed. Two-tailed Student's *t*-tests were performed when comparing two samples. Values of $P \leq 0.05$ were considered significant differences.

3. Results

3.1. Cloning and sequencing of hamster lipin 1α and lipin 1β

Loss of GPI activity in mutants previously reported by this laboratory resulted in decreased PAP activity and greatly reduced glycerolipid biosynthesis [5]. We wanted to test if we could overcome this glycerolipid biosynthetic deficiency in the GPI deficient mutants by overexpression of either lipin 1α or lipin 1β. We cloned and sequenced hamster lipin 1 in these cells using primers designed to regions of high identity with known lipin 1 cDNA sequences from other species. Initial sequencing was performed using PCR products obtained from total RNA isolated from wild-type CHO-K1 cells. Homology alignment identified this sequence as the lipin 1β isoform (*Lpin 1β*, GenBank accession no. GU474204) (Fig. 2). Since sequences were obtained from PCR products, this suggests that lipin 1β is the major form of lipin 1 in CHO-K1 cells.

Minor sequencing chromatogram peaks at the beginning of the beta β-insert suggested the presence of another isoform being expressed in lower abundance in CHO-K1. The β-insert contains a unique Ale I restriction site. Therefore, we treated our PCR product with this endonuclease to specifically digest the beta isoform. Gel purification of the digest-resistant DNA allowed us to clone and sequence the *Lpin 1α* isoform (GenBank accession no. GU474205).

Similar to the lipin 1β from other species, hamster lipin 1β contained an additional insert of 39 amino acids (β-insert; Fig. 2) when compared to the lipin 1α isoform. The hamster lipin 1 displayed high identity with lipin 1 sequences from mouse (93.8%), rat (94.4%) and human (89.5%). It contained all the features found in the lipin family (Fig. 2) including the NLS signal, the HAD-like domain and two highly homologous regions known as N-terminal and C-terminal lipin domains (NLIP and CLIP). However, some features distinct to the hamster sequence were also found. The beta insert is slightly longer, by seven amino acids, compared to mouse and rat (Fig. 2). All of the nineteen residues, identified by mass spectrometry to be phosphorylated in mouse lipin 1 [12], were retained in the hamster sequence except for Ser-392, which is a leucine residue. This residue is also replaced by a leucine for the human form of lipin 1, indicating perhaps that the phosphorylation of Ser-392 is not of importance for the regulation of lipin 1.

Like the CHO-K1 cells, cloning and sequencing of hamster lipin 1 from the cell lines ZR-82 and GroD1 also suggested that lipin 1β was the most abundant alternative spliced isoform for these cells. Sequencing of both lipin 1α and lipin 1β from the GPI-deficient mutant, GroD1, showed 100% identity with the CHO-K1 sequence, demonstrating that there were no mutations associated with the lipin 1α or lipin 1β cDNA in this cell line.

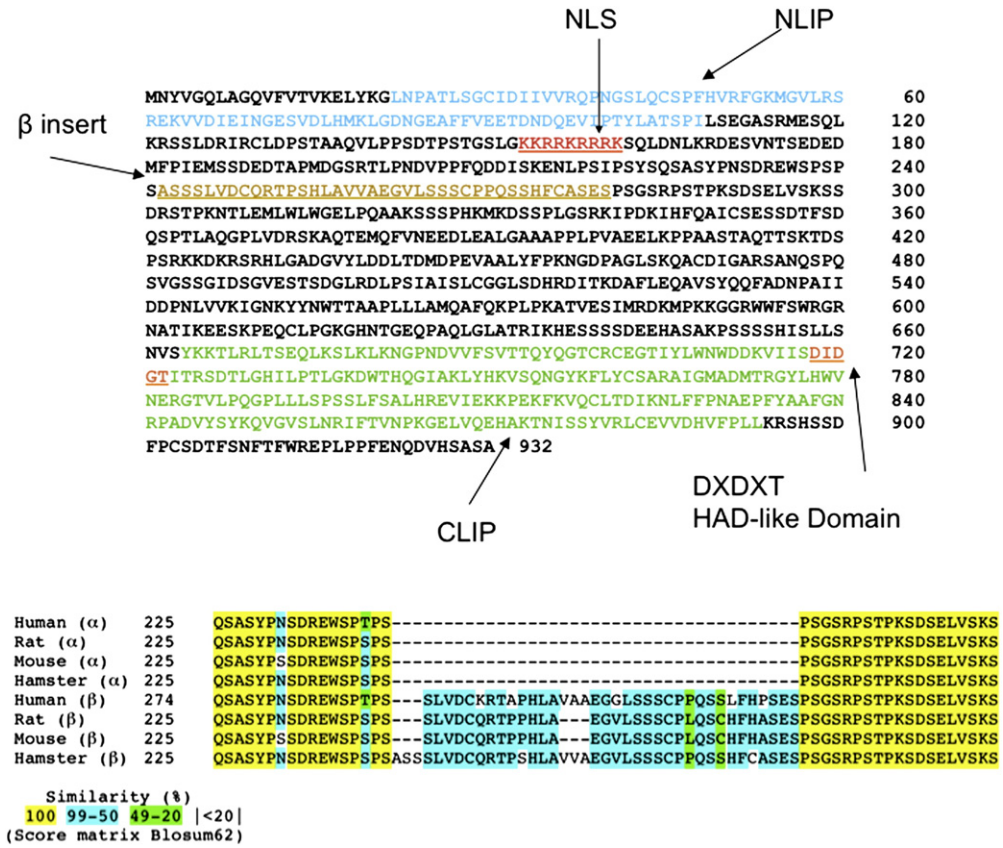

Fig. 2. Sequence and features of hamster lipin 1. Top panel: Amino acid sequence of Chinese hamster lipin 1β. Arrows and colors indicate protein features: NLIP and CLIP, N-terminal and C-terminal lipin domains as determined by homology with other known lipin sequences; NLS, nuclear localization sequence; HAD (haloacid dehalogenase)-like motif; In gold, β-insert of 39 amino acids. Lower panel: Alignment of the new sequence with respect to known lipin 1 at the beta-insert region showing the high identity and similarities between sequences.

3.2. Overexpression of lipin 1 in the GPI mutant GroD1 yields high in-vitro PAP activity, but does not correct the glycerolipid biosynthetic deficiency

To test if the overexpression of hamster lipin 1 could revert the phenotype observed in GroD1 cells (i.e., deficiency in PAP activity, reduced glycerolipid biosynthesis and temperature-sensitive growth phenotype) we stably expressed hamster lipin 1α and lipin 1β in the mutant cell line, GroD1 and the parent cell line ZR-82 using the retroviral vector pBABEpuro [19]. After selection with puromycin, we examined the surviving population for expression of hamster lipin 1 by assaying PAP activity in the soluble fraction of lysed cells. Cells transfected with lipin 1α and lipin 1β displayed approximately a 6-fold higher PAP activity than the activity normally found in ZR-82 cells (Fig. 3A).

Despite the higher PAP activity in these cells, overexpression of either lipin 1α or 1β did not revert the temperature sensitive growth phenotype of GroD1 (Fig. 3B). Phospholipid synthesis, assessed using short-term $^{32}P_i$ incorporation into phospholipids [5], showed that ZR-82 overexpressing lipin 1α (ZR-82$^{t(Lpin1\alpha)}$) presented higher $^{32}P_i$ incorporation into phospholipids (Fig. 4A), primarily due to a 1.4-fold increase in PC labeling. This was accompanied by a statistically significant decrease in PA, PI and PG labeling. ZR-82 cells over-expressing lipin 1β (ZR-82$^{t(Lpin1\beta)}$) did not present any significant differences compared to uninfected ZR-82 cells with respect to $^{32}P_i$ labeling. For GroD1 cells, overexpression of either lipin 1 isoform (GroD1t$^{(Lpin1\alpha)}$ and GroD1$^{t(Lpin1\beta)}$) did not change the incorporation of $^{32}P_i$ into the general phospholipid pool. There was only a minor (<15%), but statistically significant, increase in PC labeling in GroD1$^{t(Lpin1\alpha)}$ cells compared to uninfected GroD1 cells (Fig. 4B).

Since CHO cells do not accumulate significant triglyceride levels under normal growth conditions, we supplemented the medium with 100 μM oleic acid to force their accumulation. While an increase in triglyceride levels in cells may reflect an increase in synthesis or a decrease in lipolysis or both, the accumulation of triglycerides in cells indicates a shift favoring synthesis. When ZR-82 cells were grown for 2 days under these conditions they accumulated triglycerides (Fig. 4C). Infection of these cells with either lipin 1α or lipin 1β was unable to affect the levels of neutral lipids. When grown under the same conditions, GroD1 cells accumulated much less triglyceride than ZR-82 cells (Fig. 4D). Instead, their cholesterol ester levels were enhanced roughly two-fold over those of the parent strain. GroD1$^{t(Lpin1\alpha)}$ contained about 10% less cholesterol esters compared to cells infected with the vector only (GroD1$^{t(Puro)}$). No statistically significant differences were observed for other glycerolipids assayed in GroD1 cells expressing hamster lipin 1α or lipin 1β (Fig. 4B and D).

In summary, overexpression of lipin 1 isoforms in GroD1 increased PAP activity measured in the soluble fraction of cell homogenates, but had no dramatic effect on glycerolipid synthesis. Taken together this strongly supports the notion that, in the mutant cell line, the mutation in GPI is the cause of the deficiency in glycerolipid biosynthesis, and this cannot be overcome by increased PAP expression/activity.

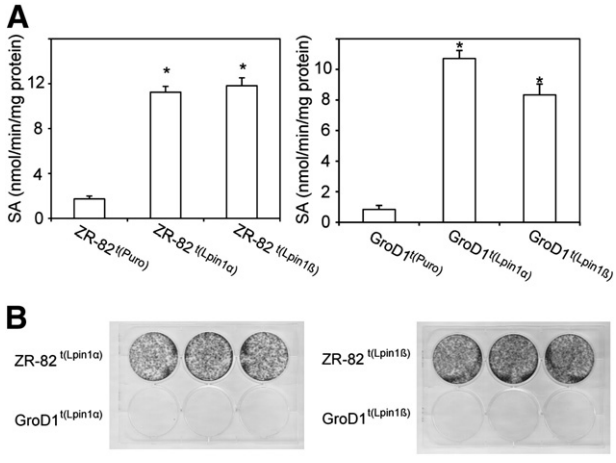

Fig. 3. PAP activity and cell growth in ZR-82 and GroD1 cells expressing lipin 1 isoforms. Cells stably expressing hamster lipin 1α, superscript t(Lpin1α), or lipin 1β, superscript t (Lpin1β), were engineered using retroviral constructs as described in Material and methods. (A) PAP activity was measured as Mg^{2+}-dependent release of water-soluble $^{32}P_i$ from chloroform-soluble [^{32}P]PA in soluble cell fractions [22]. (B) Cells stably expressing lipin 1 isoforms were plated at 3×10^4 cells/well in six well plates and grown at 40 °C for 10 days, followed by staining with Coomassie blue. Graph values represent the average ± standard deviation of three independent experiments. *Indicates a $P\leq0.05$ that the value for each cell infected with either lipin 1 isoform is the same the value obtain by infecting the same cell with an empty vector.

3.3. Decreasing glucose and increasing serum levels in the growth medium restores growth and phospholipid biosynthesis

All of our CHO-derived cell lines are typically grown in Ham's F12 medium, which contains 10 mM glucose and is supplemented with 10% FBS. GroD1 cells display a temperature-sensitive growth phenotype, their growth ceasing after two doublings at 40 °C [5]. The cause of this growth phenotype was not known. We altered medium components in an effort to restore growth at 40 °C. Reduction of glucose levels in the medium with 10% FBS partially rescued GroD1 cells at 40 °C with maximum cell growth between 2 and 4 mM glucose (Fig. 5A). Increasing FBS levels also had a significant effect on cell growth at the non-permissive temperature, partially rescuing the GroD1 cells even in the presence of inhibitory levels of glucose (10 mM). However, increased serum levels failed to recover growth at 25 mM glucose indicating sensitivity to glucose in the GPI-deficient state.

We measured phospholipid biosynthesis at 40 °C using medium that yielded optimal growth of GroD1 (6 mM glucose and 30% FBS) and the normal medium (10 mM glucose and 10% FBS). Using the optimal growth medium, not only was the incorporation of $^{32}P_i$ labeling into total lipids increased, but the incorporation of label into PC, PE and PA were also restored nearer to the levels expected of ZR-82 cells (Fig. 5B).

To explore the reason for the glucose sensitivity we measured the levels of glucose-6-phosphate (G6P) and fructose-6-phosphate (F6P) in perchloric acid extracts of GroD1 and ZR-82 cells in order to see if there was a change in these two glycolytic intermediates, products and substrates of the reversible reaction catalyzed by GPI. Both cell lines presented similar levels of F6P (Fig. 5C) however GroD1 cells accumulated G6P to one order of magnitude higher than ZR-82 cells (Fig. 5C). This indicates that a new steady state was achieved for these metabolites in GroD1, with a large accumulation of G6P as a consequence of the GPI mutation.

3.4. Akt/mTOR signaling in GroD1 and ZR-82 cells

PAP/Lipin 1 has been shown to be under the control of the mTOR pathway [10]. Furthermore, the mTOR pathway is known to be a nutrient signaling pathway [25,26]. Hence, we explored the activation of several members of the Akt/mTOR pathway using Western blot analysis in cell lysates from ZR-82 and GroD1 cells.

PDK1 is an important mediator of insulin-stimulated mTOR activation [27]. No statistically significant difference was observed in the phosphorylation level of Ser 241 on PDK1 in lysates from ZR-82 and GroD1 (Fig. 6). However, we found that, in the same lysates, residue Thr 308 of Akt, a substrate of PDK1, presented higher phosphorylation levels (about 4-fold) in GroD1 cells compared to ZR-82. In addition, Akt residue Ser 473 and S6K Thr 389, both specific substrates of the mTOR complex [26,27], had increased phosphorylation levels in GroD1, about 2-fold over ZR-82. We observed no differences in the phosphorylation levels of either mTOR, Ser 2482 or

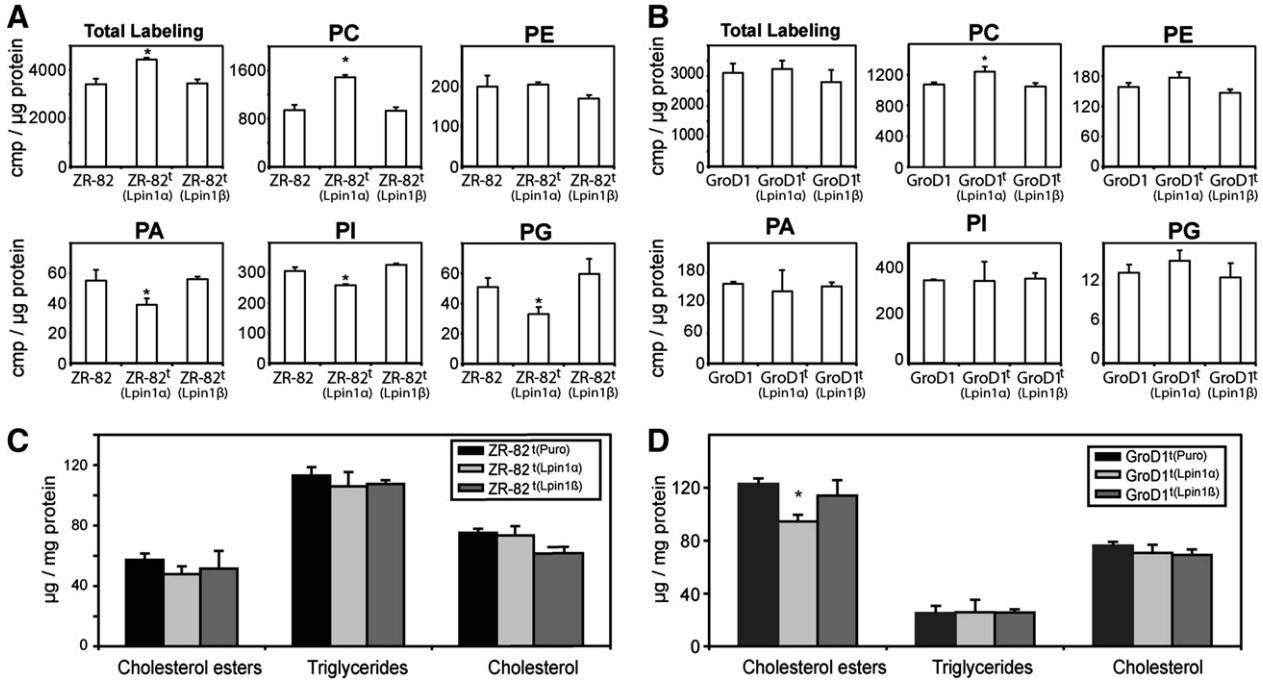

Fig. 4. Effects of over-expression of hamster lipin 1 in ZR-82 and GroD1 cells on glycerolipid synthesis. Cells stably expressing hamster lipin 1α, t(Lpin1α), or lipin 1β, t(Lpin1β), were engineered using retroviral constructs as describe in Material and Methods. (A) and (B) phospholipid biosynthesis, measured by short-term labeling with $^{32}P_i$ (2 h at 40 °C), followed by 2D-TLC separation and quantification by liquid scintillation spectrometry. (C) and (D) Cholesterol ester, triglyceride and cholesterol levels after 48 h in medium supplemented with 100 µM oleic acid, measured after TLC separation by densitometric quantitation of charred pates. For all graphs, values represent the average ± standard deviation of three independent samples. *Indicates a $P \leq 0.05$ that the value is the same as the value obtained from uninfected or vector-alone infected cells.

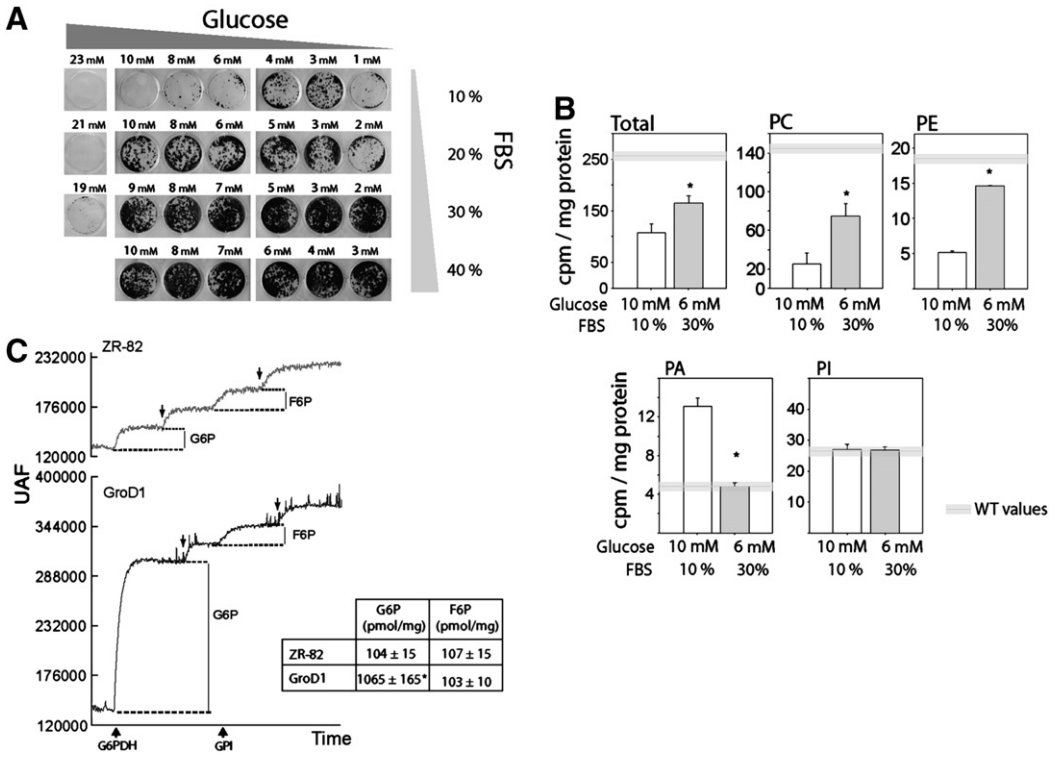

Fig. 5. Glucose and fetal bovine serum concentrations effects on temperature sensitive growth and phospholipid biosynthesis of GroD1 cells. (A) Coomassie blue colony staining of GroD1 cells grown in media containing the indicated amounts of glucose and FBS at 40 °C for 14 days. Increasing amounts of FBS, as well as lower concentrations of glucose allowed GroD1 growth at the restrictive temperatures. (B) Phospholipid biosynthesis of GroD1 cells at the indicated glucose and FBS concentrations. Cells were labeled with $^{32}P_i$ for 2 h at 40 °C, lipids were extracted, separated and quantified as described in Material and Methods. The horizontal bars represent expected values for parent strain ZR-82. All glucose values took into account the contribution of the fetal bovine serum used to supplement the medium which contains 8 mM glucose. (C) Fluorescent measurement of cellular glucose-6-phosphate (G6P) and fructose-6-phosphate (F6P) cellular levels. Arrows on the tracing indicate that a bolus of 300 pmol of G6P or F6P standard was added. The addition of G6PDH and GPI are indicated on the X axis. Insert: Quantitated metabolites levels. All values represent the average ± standard deviation of three independent experiments. *Indicates a $P \leq 0.05$ between samples.

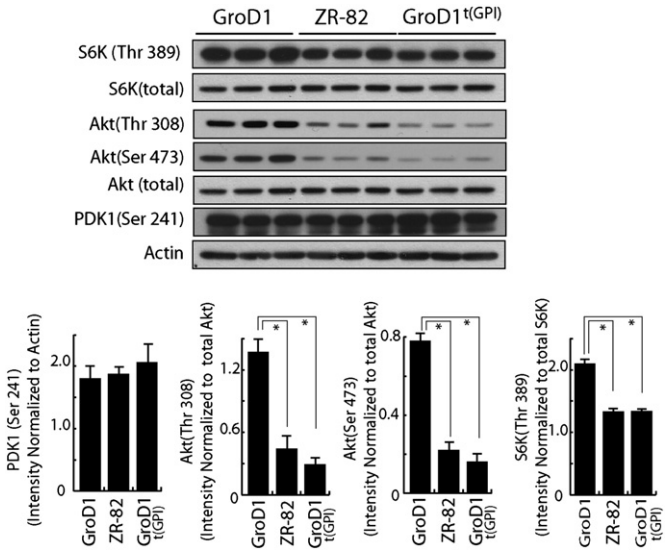

Fig. 6. GPI-deficiency results in mTOR substrates hyperphosphorylation. GroD1, ZR-82 and Grod1$^{t(GPI)}$ (GroD1 stably expressing GPI) cells were plated in six well plates (8×10^4 cells/well), allowed to attach overnight at 33 °C, then shifted to 40 °C for 24 h. Cell lysates were collected in RIPA buffer and subject to Western blot analysis using phospho-specific antibodies. Densitometry analyses are shown below the blots. Values represent the averages of three independent experiments. *$P\leq0.05$ between the indicated samples using Tukey's HSD multiple comparison procedure.

Ser 2448 (Table 1). We found no statistically significant difference in the phosphorylation levels of other members of the Akt signaling pathway including PTEN, GSK-3β and cRaf (Table 1). Additionally, we assayed for activation of AMPK, a Ser/Thr kinase, which senses cellular energy ATP/AMP levels [28]. We found no increased phosphorylation of the AMPK α subunit (Table 1).

Altogether, these results suggest that there is a PDK1 independent activation of the nutrient-signaling mTOR pathway in GroD1 cells compared to ZR-82. This activation is concomitant with a non-phosphorylation-mediated activation of the mTOR complex in these cells.

3.5. GroD1 cells do not localize lipin 1α to the nucleus

As mentioned earlier, all lipin members contain a NLS (nuclear localization signal). Fluorescence microscopy [8] and immunofluorescence microscopy [11] have shown that lipin 1α is predominantly present in the nucleus. On the other hand, the alternatively spliced form, lipin 1β, is mainly cytoplasmic.

We fused GFP to the C-terminus of lipin 1α and lipin 1β and transfected ZR-82 and GroD1 with these constructs. There was a significant difference in subcellular localization of lipin 1α-GFP when comparing the two cell lines. For the parent strain, ZR-82, lipin 1α-GFP presented strong fluorescence in the nuclei (Fig. 7A), in accordance with previous findings [11]. Strikingly, in GroD1 cells expressing the lipin 1α-GFP construct most of the fluorescence was restricted to the cytosol. We quantified the cellular distribution of lipin 1α-GFP by analyzing co-localization with the nuclear fluorescent stain Hoechst. Twenty-four hours post-transfection, 87% of ZR-82 cells presented fluorescence in their nuclei, while only 23% of GroD1 cells had the expected fluorescence distribution for lipin 1α (Fig. 7B).

Co-expression of wild-type GPI with the lipin 1α-GFP construct restored nuclear localization of lipin 1α in GroD1; 76% of these cells presented nuclear fluorescence. This suggests that the mislocalization of lipin 1α in GroD1 is a result of the GPI mutation and links abnormal subcellular localization of lipin 1α to the glycerolipid biosynthesis deficiency observed in the GPI-deficient cell line [5]. As further evidence that abnormal mTOR activation is preventing lipin 1α from proper localization in GroD1, we treated cells with the mTOR inhibitor, rapamycin [10]. This treatment also resulted in lipin 1α association with the nucleus (Fig. 7B).

To investigate the effects of glucose sensitivity on lipin 1α localization in GroD1 cells, we grew the cells with medium containing reduced glucose (4 mM) and 30% FBS, conditions which favored growth of this cell line at 40 °C. GroD1 cells grown in this medium showed a significant increase in the nuclear localization of lipin 1α (Fig. 7B).

It is thought that the lipin 1β isoform is directly involved in glycerolipid biosynthesis ([29,30]). In both ZR-82 and GroD1, the fusion protein, lipin 1β-GFP displayed a diffuse extranuclear fluorescence consistent with a cytoplasmic protein (Fig. 8A). Less than 25% of the cells from either cell line displayed nuclear fluorescence when transfected with lipin 1β-GFP (Fig. 8B). It was impossible to tell whether the lipin 1β-GFP was more, or less membrane-associated in the GroD1 cells, although the fluorescence in the ZR-82 cells appeared to be more localized in the perinuclear region. Lipin 1 is also a known target of mTOR ([10,13,31]) and phosphorylation of lipin 1β prevents its membrane association and therefore its ability to participate in glycerolipid synthesis. Western analyses of lysates from cells transfected with the lipin 1β-GFP fusion construct were run. ZR-82 and GroD1 displayed different migration patterns (Fig. 8C). As observed previously for lipin 1β ([12,13]), there appeared to be more than one species of the protein, the slower migrating species representing the more heavily phosphorylated forms. While the density was evenly distributed throughout the lipin 1β-GFP species in the ZR-82 lysates, the dominant species was clearly the slowest migrating (most phosphorylated) species in GroD1. In fact, we could find no signal that co-migrated with this putatively more phosphorylated species in the ZR-82 samples.

Table 1
Phosphorylation levels of mTOR, AMPK and other members of the Akt signaling pathway.

Protein	ZR-82 (relative intensity)	GroD1 (relative intensity)	Normalized to
mTOR (Ser 2482)	0.10 ± 0.03	0.12 ± 0.02	Actin
mTOR (Ser 2448)	0.37 ± 0.09	0.47 ± 0.06	Actin
PTEN (Ser 380)	1.1 ± 0.1	1.3 ± 0.2	PTEN (total)
GSK-3β (Ser 9)	1.4 ± 0.6	1.7 ± 0.7	Actin
c-Raf (Ser 258)	4.5 ± 1.0	3.7 ± 0.5	Actin
AMPKα (Thr 178)	6.0 ± 1.2	5.2 ± 0.8	AMPKα (total)

Samples were plated into six well plates (8×10^4 cells/well), allowed to attach overnight at 33 °C, then grown at 40 °C for 24 h prior collecting cell lysate in RIPA buffer. Lysates were subject to Western blot analysis. Values represent average ± standard deviation of the densitometry analysis of three independent samples. No statistically significant ($P\leq0.05$) differences were observed between ZR-82 and GroD1.

4. Discussion

In this study we report the first cloning and sequencing of the α and β splice variants of lipin 1 from Chinese hamster cells. These hamster isoforms were similar to previously cloned lipin 1α and lipin 1β from rat [10] and mouse [11] in sequence and in cellular localization for wild-type cells. Overexpression of either form of hamster lipin 1 in CHO cells resulted in an increase in a Mg^{2+}-dependent PAP activity, indicating that these cloned sequences indeed encode an active PAP enzyme. It is interesting that, while retroviral-mediated expression of lipin 1α and lipin 1β in the GPI-deficient cells increased in-vitro PAP activity, it failed to restore TG accumulation and phospholipid biosynthesis in this mutant cell line. (Fig. 4). This confirms a pleiotropic effect of the GPI mutation or loss of GPI activity on PAP cellular activity. We have ruled out that the nature of this effect on the suppression of glycerolipid biosynthesis is related to an impairment of glycolysis, per se, since we have previously reported no reduction in ATP levels or glycerol-3-phosphate levels in the GPI mutant cell line [5]. Furthermore, we have shown that levels of the glycolytic metabolite F6P and phospho AMPK, a

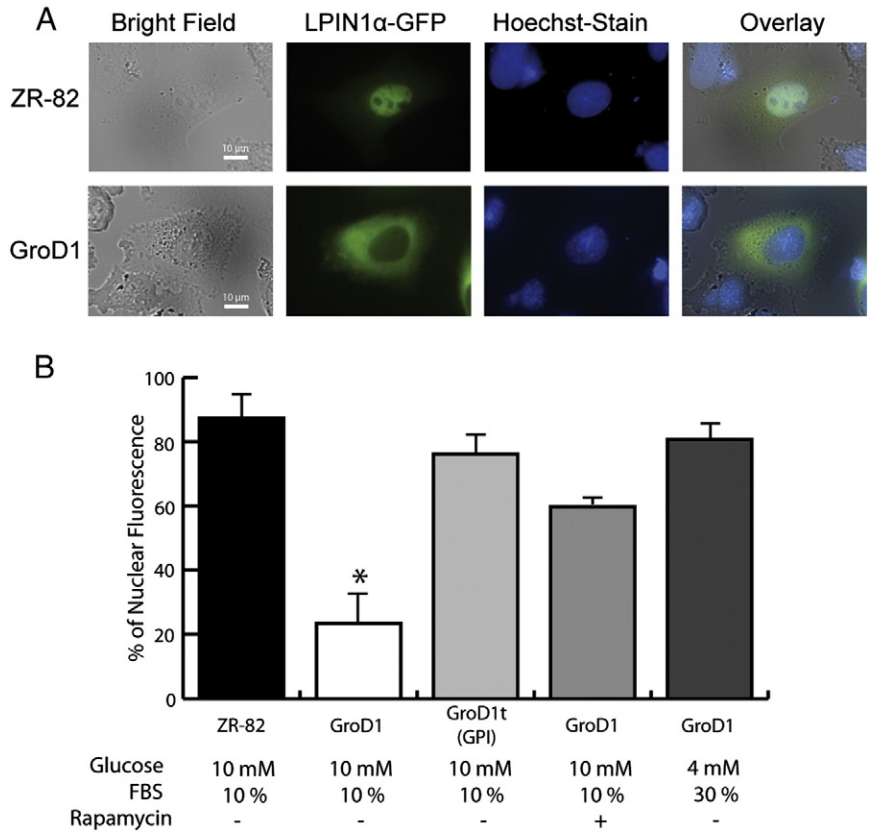

Fig. 7. GPI deficiency induces an altered lipin 1 subcellular localization dependent of the mTOR pathway and glucose/FBS media concentration. Cells were transfected with a mammalian expression vector containing human lipin 1α-GFP fusion protein. (A) Live cell images taken with a Nikon deconvolution epifluorescence microscope 24 h post-transfection. In blue, Hoechst fluorescent nuclear stain; in green, GFP fluorescence. Fluorescent images were overlaid onto a bright field image. (B) Quantitation of the cellular localization of human lipin 1α-GFP construct in ZR-82, GroD1, GroD1$^{t(GPI)}$ (GroD1 cell stably expressing wild-type GPI), as well as GroD1 cell grown in media with low glucose and high FBS or treated with 50 nM rapamycin. Each experimental condition involved analysis of over 100 cells/strain. The data bars represent the mean of three such experiments, +/− one standard deviation. All differ significantly from GroD1 under standard conditions (*$P<0.05$).

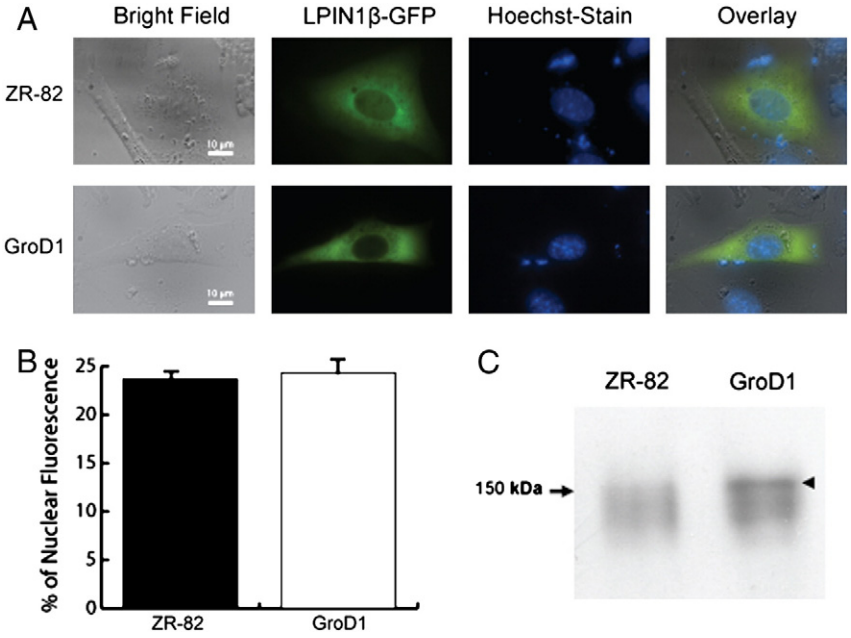

Fig. 8. Cellular localization of lipin 1β in ZR-82 and GroD1 cells. Cells were transfected with a mammalian expression vector containing human lipin 1β-GFP fusion protein. (A) Live cell images taken with a Nikon deconvolution epifluorescence microscope 24 h post-transfection. In blue, Hoechst fluorescent nuclear stain; in green, GFP fluorescence. Fluorescent images were overlaid onto a bright field image. (B) Quantitation of the cellular localization of human lipin 1β-GFP construct. (C) Western analysis performed on cell lysates using antibody to GFP as described in Materials and Methods. The arrow head on the right indicates the putative hyperphosphorylated lipin 1β-GFP species. All experiments were conducted three separate times with similar results. Values represent the average ± standard deviation of three independent experiments; each experiment involved the analysis of over 100 cells/strain. No statistically significant difference ($P \leq 0.05$) was observed or ZR-82 and GroD1 cells.

kinase that responds to changes in the ATP/AMP ratio [28], are unaltered in the mutant GroD1 when compared to the parent cell line, ZR-82.

Our evidence suggests that the reduced glycerolipid biosynthesis is a result of an abnormal activation of the nutrient signaling mTOR pathway. In order for PAP/lipin 1 to be lipogenically active, it must associate with membranes since this is where its substrate, PA, is located [12,32–34]. It has been previously demonstrated that activation of mTOR results in phosphorylation of lipin 1 [10,13,35], resulting in the sequestration of lipin 1 in the cytosol [12], thus preventing PAP access to the nucleus and membranes. Additionally, inhibition of the mTOR pathway results in membrane-association and nuclear localization of PAP/Lipin 1 [12,13]. Abnormal activation of the mTOR pathway would explain the altered subcellular distribution of lipin 1α and reduced glycerolipid biosynthesis in GroD1, as well as the observed increase in phosphorylated mTOR targets, S6K(Ser 389) and Akt(Ser 473) [26,27]. Furthermore, treatment of mutant cells with rapamycin, a well established inhibitor of the mTOR complex, [10] reverts the nuclear localization of lipin 1α. This is consistent with the notion that altered subcellular localization is a consequence of the overactivated mTOR signaling.

While lipin 1α appears to function in the nucleus as a transcription factor it is lipin 1β that is thought to be involved in glycerolipid synthesis functioning as a PAP [29]. Association with the membrane (e.g. the endoplasmic reticulum) would be required for effectiveness of this protein. Consistent with this are reports that PAP activity has been found to associate with membranes under conditions that increase glycerolipid synthesis [34]. Although the fluorescence associated with the lipin 1β-GFP fusion construct appeared to have a diffuse distribution pattern in both the parent strain and GroD1, the fluorescence in the ZR-82 cells appeared to be more localized in the perinuclear region, consistent with an association with the endoplasmic reticulum. Consistently, we did find evidence that lipin 1β is hyperphosphorylated in the mutant cells.

The GPI-deficiency resulted in accumulation of high levels of G6P, a metabolite described as an activator of the mTOR signaling pathway in isolated cardiomiocytes [36]. In addition, growth of GroD1 cells in reduced glucose medium or retroviral expression of wild-type GPI, two situations that would lower cellular levels of G6P, result in reversion of the lipogenic deficient phenotype and the abnormal subcellular localization of lipin 1α. Hence, an activated mTOR nutrient-signaling pathway, due to the accumulation of G6P, might explain the observed phenotype in GroD1 cells. Additionally, the GPI deficiency in these cells increased PA levels [5]. PA is a well established activator the mTOR signaling pathway [37]. Thus, the initial effects of G6P on mTOR activity would be exacerbated as glycerolipid biosynthesis is impaired and PA accumulates in these cells (Fig. 9).

These results have relevance to symptoms associated with human GPI deficiency. Patients with GPI deficiency present different degrees of non-spherocytic hemolytic anemia (NSHA). In some cases, these patients manifest neuromuscular dysfunctions characterized by muscle weakness and mental retardation [2,38–43]. The molecular basis for these symptoms has not been established [2]. There are 29 identified GPI mutations that cause NSHA. In all cases in which G6P levels were assayed, increased levels of this metabolite were found in red blood cells as well as in muscle and brain tissue [1,4].

Different NSHA patients present different degrees of hemolytic anemia [1]. However, the degree of the GPI deficiency does not correlate well with the severity of the anemia. For example, some patients with 60% of normal GPI activity display severe anemia [1] while patients with only 9% residual activity present with a mild to moderate anemia [44]. Interestingly, homozygous patients with the same mutation, display the same reduction in GPI activity, but display different severities of anemia [1] as well as varying degrees of neurological and muscular dysfunction [3]. Hence, it has been proposed that there must be either secondary genetic influences or environmental factors involved in the severity of the symptoms

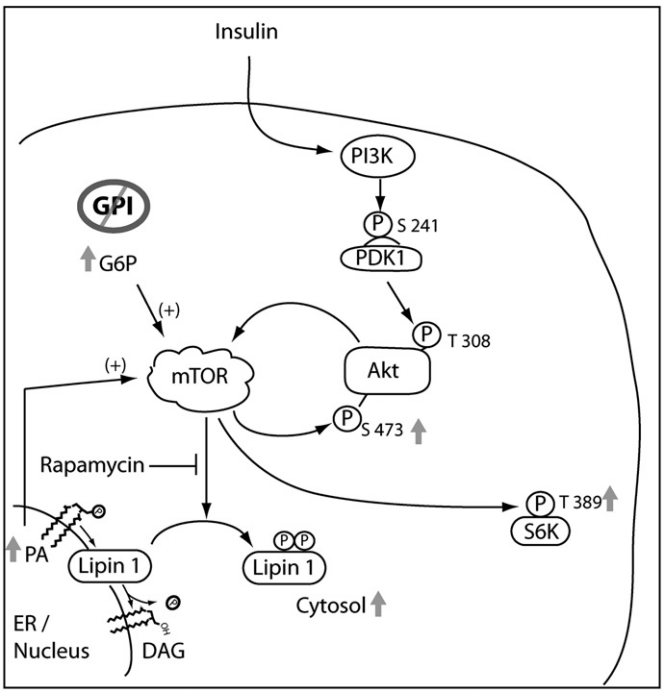

Fig. 9. Schematic diagram depicting the possible pathophysiological state of GPI-deficient GroD1 cells. The figure shows the canonical insulin/mTOR regulation of lipin 1 [10,13]. The GPI deficient cell, GroD1, accumulates G6P, a putative activator of mTOR [36]. An activated mTOR leads to cytosolic localization of lipin 1 [13]. No longer associated with membranes and away from it substrate, lipin 1 is inefficient for lipogenic synthesis. The GPI-deficient cells develop glycerolipid deficiency with accumulation of PA, another activator of mTOR [37]. Thus, exacerbating the mTOR activation. Gray arrows indicate the observation found in GroD1 cells compared to ZR-82 cells (i.e. high levels of PA and G6P, increase in phosphorylation of mTOR substrates, Akt(Ser473) and S6K(Thr389), and cytosolic presence of lipin 1).

associated with NSHA disease [1]. Perhaps our observation with respect to the glucose-dependent growth inhibition and the observed G6P accumulation may help to explain the differences in the severity in human patients and might warrant future in vivo studies to test the hypothesis that altering metabolite levels in patients with inherited GPI deficiency could alleviate the severity of symptoms.

It is interesting to note that similar symptoms are associated with GPI deficiencies and lipin mutations. For instance, GPI-deficient patients can present with mental retardation and neurological impairment that affects the brain and the spinal cord [38–43,45]. Similarly, lipin 1 mutant mice present peripheral neuropathies accompanied by demyelination, mediated by PA accumulation in Schwann cells [14,15]. Additionally, while human patients with lipin 1 mutations manifest generalized muscular hypotonia due to an alteration in the phospholipid composition of the skeletal muscle fibers [16], similar symptoms are present in human patients with the "GPI Homburg" mutation, which results in muscle weakness with histologically disproportioned muscle fibers [38]. Finally, "Majeed Syndrome", which is due to mutations in lipin 2, is characterized by recurrent anemia, due to inefficiency of the bone marrow to produce rapidly dividing erythrocyte progenitor cells [17]. Abnormalities in the red blood cell membrane lipid composition have been reported in inherited erythrocyte metabolic disorders [46]. Alteration in the membrane lipid composition should compromise cell permeability and viability. Hence, it is conceivable that the traits observed in our GPI-deficient cells might help explain some of the manifestations observed in GPI deficient mice and human patients. The neuromuscular abnormalities and the anemia could be caused by dysfunction in lipid biosynthesis, a hypothesis that needs to be examined in the future.

5. Conclusion

In summary, we report, for the first time, a pathophysiological state, GPI deficiency, in which a mutation in a glycolytic enzyme results in glucose sensitivity and a constitutive activation of the nutrient signaling mTOR pathway. Such a situation results in abnormal distribution of the lipin 1α, and possibly lipin 1β, proteins important for glycerolipid biosynthesis. These findings highlight the metabolic communication between glucose and lipid metabolism and are consistent with the known mechanism for the crosstalk between these two pathways. They may also explain some of the symptoms associated with inherited GPI deficiency, the variable severity of symptoms displayed by these patients and importantly, may offer new therapies.

Acknowledgments

This work was supported in part from a Pilot and Feasibility project from the Boston Obesity Nutrition Research Center (Grant DK46200).

References

[1] W. Kugler, M. Lakomek, Glucose-6-phosphate isomerase deficiency, Baillieres Best Pract. Res. Clin. Haematol. 13 (2000) 89–101.
[2] W. Kugler, K. Breme, P. Laspe, H. Muirhead, C. Davies, H. Winkler, W. Schroter, M. Lakomek, Molecular basis of neurological dysfunction coupled with haemolytic anaemia in human glucose-6-phosphate isomerase (GPI) deficiency, Hum. Genet. 103 (1998) 450–454.
[3] J.J. Hutton, R.R. Chilcote, Glucose phosphate isomerase deficiency with hereditary nonspherocytic hemolytic anemia, J. Pediatr. 85 (1974) 494–497.
[4] S. Merkle, W. Pretsch, Glucose-6-phosphate isomerase deficiency associated with nonspherocytic hemolytic anemia in the mouse: an animal model for the human disease, Blood 81 (1993) 206–213.
[5] J.F. Haller, C. Smith, D. Liu, H. Zheng, K. Tornheim, G.S. Han, G.M. Carman, R.A. Zoeller, Isolation of novel animal cell lines defective in glycerolipid biosynthesis reveals mutations in glucose-6-phosphate isomerase, J. Biol. Chem. 285 (2010) 866–877.
[6] J. Donkor, M. Sariahmetoglu, J. Dewald, D.N. Brindley, K. Reue, Three mammalian lipins act as phosphatidate phosphatases with distinct tissue expression patterns, J. Biol. Chem. 282 (2007) 3450–3457.
[7] G.S. Han, W.I. Wu, G.M. Carman, The Saccharomyces cerevisiae Lipin homolog is a Mg2+−dependent phosphatidate phosphatase enzyme, J. Biol. Chem. 281 (2006) 9210–9218.
[8] M. Peterfy, J. Phan, P. Xu, K. Reue, Lipodystrophy in the fld mouse results from mutation of a new gene encoding a nuclear protein, lipin, Nat. Genet. 27 (2001) 121–124.
[9] B.N. Finck, M.C. Gropler, Z. Chen, T.C. Leone, M.A. Croce, T.E. Harris, J.C. Lawrence Jr., D.P. Kelly, Lipin 1 is an inducible amplifier of the hepatic PGC-1alpha/PPARalpha regulatory pathway, Cell Metab. 4 (2006) 199–210.
[10] T.A. Huffman, I. Mothe-Satney, J.C. Lawrence Jr., Insulin-stimulated phosphorylation of lipin mediated by the mammalian target of rapamycin, Proc. Natl. Acad. Sci. U.S.A. 99 (2002) 1047–1052.
[11] M. Peterfy, J. Phan, K. Reue, Alternatively spliced lipin isoforms exhibit distinct expression pattern, subcellular localization, and role in adipogenesis, J. Biol. Chem. 280 (2005) 32883–32889.
[12] T.E. Harris, T.A. Huffman, A. Chi, J. Shabanowitz, D.F. Hunt, A. Kumar, J.C. Lawrence Jr., Insulin controls subcellular localization and multisite phosphorylation of the phosphatidic acid phosphatase, lipin 1, J. Biol. Chem. 282 (2007) 277–286.
[13] M. Peterfy, T.E. Harris, N. Fujita, K. Reue, Insulin-stimulated interaction with 14-3-3 promotes cytoplasmic localization of lipin-1 in adipocytes, J. Biol. Chem. 285 (2010) 3857–3864.
[14] C.A. Langner, E.H. Birkenmeier, K.A. Roth, R.T. Bronson, J.I. Gordon, Characterization of the peripheral neuropathy in neonatal and adult mice that are homozygous for the fatty liver dystrophy (fld) mutation, J. Biol. Chem. 266 (1991) 11955–11964.
[15] K. Nadra, A.S. de Preux Charles, J.J. Medard, W.T. Hendriks, G.S. Han, S. Gres, G.M. Carman, J.S. Saulnier-Blache, M.H. Verheijen, R. Chrast, Phosphatidic acid mediates demyelination in Lpin1 mutant mice, Genes Dev. 22 (2008) 1647–1661.
[16] A. Zeharia, A. Shaag, R.H. Houtkooper, T. Hindi, P. de Lonlay, G. Erez, L. Hubert, A. Saada, Y. de Keyzer, G. Eshel, F.M. Vaz, O. Pines, O. Elpeleg, Mutations in LPIN1 cause recurrent acute myoglobinuria in childhood, Am. J. Hum. Genet. 83 (2008) 489–494.
[17] P.J. Ferguson, S. Chen, M.K. Tayeh, L. Ochoa, S.M. Leal, A. Pelet, A. Munnich, S. Lyonnet, H.A. Majeed, H. El-Shanti, Homozygous mutations in LPIN2 are responsible for the syndrome of chronic recurrent multifocal osteomyelitis and congenital dyserythropoietic anaemia (Majeed syndrome), J. Med. Genet. 42 (2005) 551–557.
[18] R.A. Zoeller, C.R. Raetz, Isolation of animal cell mutants deficient in plasmalogen biosynthesis and peroxisome assembly, Proc. Natl. Acad. Sci. U.S.A. 83 (1986) 5170–5174.
[19] J.P. Morgenstern, H. Land, Advanced mammalian gene transfer: high titre retroviral vectors with multiple drug selection markers and a complementary helper-free packaging cell line, Nucleic Acids Res. 18 (1990) 3587–3596.
[20] E.G. Bligh, W.J. Dyer, A rapid method of total lipid extraction and purification, Can. J. Biochem. Physiol. 37 (1959) 911–917.
[21] W.S. Rasband, ImageJ, http://rsb.info.nih.go/ij/National Institute of Health Bethesda, Maryland, USA, 1997–2008.
[22] G.M. Carman, Y.P. Lin, Phosphatidate phosphatase from yeast, Methods Enzymol. 197 (1991) 548–553.
[23] H. Zheng, R.I. Duclos Jr., C.C. Smith, H.W. Farber, R.A. Zoeller, Synthesis and biological properties of the fluorescent ether lipid precursor 1-O-[9'-(1''-pyrenyl)] nonyl-sn-glycerol, J. Lipid Res. 47 (2006) 633–642.
[24] G. Lang, G. Michal, D-Glucose-6-phosphate and D-Fructose-6-phosphate, Methods of Enzymatic Analysis, Second Edition III (1974) 1238–1242.
[25] P.B. Dennis, A. Jaeschke, M. Saitoh, B. Fowler, S.C. Kozma, G. Thomas, Mammalian TOR: a homeostatic ATP sensor, Science 294 (2001) 1102–1105.
[26] P. Gulati, G. Thomas, Nutrient sensing in the mTOR/S6K1 signalling pathway, Biochem. Soc. Trans. 35 (2007) 236–238.
[27] D.D. Sarbassov, D.A. Guertin, S.M. Ali, D.M. Sabatini, Phosphorylation and regulation of Akt/PKB by the rictor-mTOR complex, Science 307 (2005) 1098–1101.
[28] D. Carling, V.A. Zammit, D.G. Hardie, A common bicyclic protein kinase cascade inactivates the regulatory enzymes of fatty acid and cholesterol biosynthesis, FEBS Lett. 223 (1987) 217–222.
[29] K. Reue, D.N. Brindley, Thematic Review Series: Glycerolipids. Multiple roles for lipins/phosphatidate phosphatase enzymes in lipid metabolism, J. Lipid Res. 49 (2008) 2493–2503.
[30] G.M. Carman, G.S. Han, Roles of phosphatidate phosphatase enzymes in lipid metabolism, Trends Biochem. Sci. 31 (2006) 694–699.
[31] D. Ryu, K.J. Oh, H.Y. Jo, S. Hedrick, Y.N. Kim, Y.J. Hwang, T.S. Park, J.S. Han, C.S. Choi, M. Montminy, S.H. Koo, TORC2 regulates hepatic insulin signaling via a mammalian phosphatidic acid phosphatase, LIPIN1, Cell Metab. 9 (2009) 240–251.
[32] S.J. Taylor, E.D. Saggerson, Adipose-tissue Mg2+−dependent phosphatidate phosphohydrolase. Control of activity and subcellular distribution in vitro and in vivo, Biochem. J. 239 (1986) 275–284.
[33] R.A. Pittner, R. Fears, D.N. Brindley, Interactions of insulin, glucagon and dexamethasone in controlling the activity of glycerol phosphate acyltransferase and the activity and subcellular distribution of phosphatidate phosphohydrolase in cultured rat hepatocytes, Biochem. J. 230 (1985) 525–534.
[34] C. Cascales, E.H. Mangiapane, D.N. Brindley, Oleic acid promotes the activation and translocation of phosphatidate phosphohydrolase from the cytosol to particulate fractions of isolated rat hepatocytes, Biochem. J. 219 (1984) 911–916.
[35] N. Grimsey, G.S. Han, L. O'Hara, J.J. Rochford, G.M. Carman, S. Siniossoglou, Temporal and spatial regulation of the phosphatidate phosphatases lipin 1 and 2, J. Biol. Chem. 283 (2008) 29166–29174.
[36] S. Sharma, P.H. Guthrie, S.S. Chan, S. Haq, H. Taegtmeyer, Glucose phosphorylation is required for insulin-dependent mTOR signalling in the heart, Cardiovasc. Res. 76 (2007) 71–80.
[37] Y. Fang, M. Vilella-Bach, R. Bachmann, A. Flanigan, J. Chen, Phosphatidic acid-mediated mitogenic activation of mTOR signaling, Science 294 (2001) 1942–1945.
[38] W. Schroter, S.W. Eber, A. Bardosi, M. Gahr, M. Gabriel, F.C. Sitzmann, Generalised glucosephosphate isomerase (GPI) deficiency causing haemolytic anaemia, neuromuscular symptoms and impairment of granulocytic function: a new syndrome due to a new stable GPI variant with diminished specific activity (GPI Homburg), Eur. J. Pediatr. 144 (1985) 301–305.
[39] S.W. Eber, M. Gahr, M. Lakomek, G. Prindull, W. Schroter, Clinical symptoms and biochemical properties of three new glucosephosphate isomerase variants, Blut 53 (1986) 21–28.
[40] E. Beutler, C. West, H.A. Britton, J. Harris, L. Forman, Glucosephosphate isomerase (GPI) deficiency mutations associated with hereditary nonspherocytic hemolytic anemia (HNSHA), Blood Cells Mol. Dis. 23 (1997) 402–409.
[41] A. Kahn, H.A. Buc, R. Girot, D. Cottreau, C. Griscelli, Molecular and functional anomalies in two new mutant glucose-phosphate-insomerase variants with enzyme deficiency and chronic hemolysis, Hum. Genet. 40 (1978) 293–304.
[42] A. Zanella, C. Izzo, P. Rebulla, L. Perroni, M. Mariani, G. Canestri, G. Sansone, G. Sirchia, The first stable variant of erythrocyte glucose-phosphate isomerase associated with severe hemolytic anemia, Am. J. Hematol. 9 (1980) 1–11.
[43] O. Shalev, R.S. Shalev, L. Forman, E. Beutler, GPI Mount Scopus–a variant of glucosephosphate isomerase deficiency, Ann. Hematol. 67 (1993) 197–200.
[44] H. Kanno, H. Fujii, A. Hirono, Y. Ishida, S. Ohga, Y. Fukumoto, K. Matsuzawa, S. Ogawa, S. Miwa, Molecular analysis of glucose phosphate isomerase deficiency associated with hereditary hemolytic anemia, Blood 88 (1996) 2321–2325.
[45] P.W. Helleman, J.P. Van Biervliet, Haematological studies in a new variant of glucosephosphate isomerase deficiency (GPI Utrecht), Helv. Paediatr. Acta 30 (1976) 525–536.
[46] G.J. Brewer, Inherited erythrocyte metabolic and membrane disorders, Med. Clin. North Am. 64 (1980) 579–596.